

## Hydrazine Fuels for Bimetallic Catalytic Microfluidic Pumping

Michael E. Ibele, Yang Wang, Timothy R. Kline, Thomas E. Mallouk,\* and Ayusman Sen\*

Department of Chemistry and Center for Nanoscale Science, The Pennsylvania State University,  
University Park, Pennsylvania 16802

Received April 16, 2007; E-mail: asen@psu.edu; tom@chem.psu.edu

The problem of controlling fluid flow on the micro- and nano-length scales is important in microanalysis, nanoparticle assembly, and other emerging applications. We and others have demonstrated autonomous nanoparticle movement and micrometer-scale fluid flow driven by the asymmetric catalytic decomposition of hydrogen peroxide over bimetallic surfaces.<sup>1–7</sup> Movement on larger length scales has also been reported both by using diodes to rectify an external ac electric field and by employing the combination of glucose and oxygen as fuel.<sup>8,9</sup> Here we report that the electrocatalytic mechanism proposed by our group and Mano and Heller for energy transduction is general and can be extended to other fuels.<sup>5–6,9</sup> Furthermore, it is now possible to control the *direction* of fluid flow in a system via the proper choice of fuel.

The novel bimetallic fluid pumping system consists of spatially defined palladium (Pd) features on a gold (Au) surface and can incorporate two different fuels, hydrazine (N<sub>2</sub>H<sub>4</sub>) or *asym*-N,N-dimethylhydrazine (N<sub>2</sub>Me<sub>2</sub>H<sub>2</sub>). This system induces a fluid flow which was observed via the movement of silica or amidine-functionalized polystyrene tracer particles (2.34 μm and 2.1 μm diameters, respectively). Depending on the colloid ζ-potential and the fuel used, colloids were induced to flow toward or away from the palladium features along the gold surface (Figure 1).

Surfaces were prepared by using an electron beam to evaporate a thickness of 100 nm of Au (with a 10 nm adhesion layer of Cr) onto silica which had a thermally grown silicon dioxide layer. Conventional microfabrication techniques were then used to deposit circular Pd features (90 μm diameter, 100 nm thick, 10 nm Cr adhesion layer) onto the Au. An alternative surface design patterned electrically isolated Pd and Au features 10 μm apart which could then be connected externally via an insulated wire and the short circuit current measured. These surfaces were then exposed to colloid-containing solutions of 2% N<sub>2</sub>H<sub>4</sub> (611 mM; pH 11) or 50 mM N<sub>2</sub>Me<sub>2</sub>H<sub>2</sub>, prepared in deionized water (18.0 MΩ\*cm). Colloid movement was observed via an optical microscope in differential interference contrast mode and tracked using PhysVis (Kenyon College). Colloid velocities were tracked over short distances (~30 μm) where their velocities were approximately constant. ζ-Potentials in pH 11 NaOH were measured using a ZetaPALS instrument and confirmed via microelectrophoresis (pH 11 NaOH was used to mimic the N<sub>2</sub>H<sub>4</sub> solution because N<sub>2</sub>H<sub>4</sub> reacts with the ZetaPALS electrodes).

When the solution of N<sub>2</sub>H<sub>4</sub> containing silica colloids (ζ = –124(10) mV) was exposed to the surfaces, colloids at the Au surface near the Pd feature were seen to migrate inward (toward the Pd) at an average speed of 4 μm/s (Figure 2). The initial current density between the Pd and Au features in 2% N<sub>2</sub>H<sub>4</sub> was measured to be on the order of 14 A/m<sup>2</sup> with the Au acting as the cathode.

However, when silica colloids in a N<sub>2</sub>Me<sub>2</sub>H<sub>2</sub> solution were placed on the surface, the colloids were seen to move slowly outward along the Au surface at an average speed of 0.7 μm/s. The direction of current flow between the two electrodes was also reversed, with a

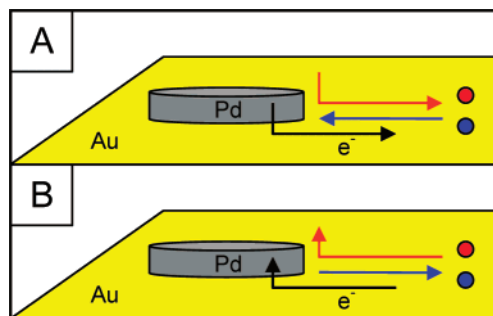


**Figure 1.** Direction of movement of silica colloids (blue), amidine-functionalized colloids (red), and electrons (black) over a Au surface relative to a Pd feature in a solution containing (a) N<sub>2</sub>H<sub>4</sub> or (b) N<sub>2</sub>Me<sub>2</sub>H<sub>2</sub>.

measured current density of approximately –1.4 A/m<sup>2</sup> with the gold acting as the anode.

When the silica colloids were replaced with amidine functionalized latex colloids (ζ = –44(10) mV), movement in the N<sub>2</sub>H<sub>4</sub> fueled system was seen in the opposite direction—outward along the Au surface at a speed of 4 μm/s. This reversal was also seen in the N<sub>2</sub>Me<sub>2</sub>H<sub>2</sub> system, as amidine colloids moved toward the Pd then up away from the surface at a speed of 2.7 μm/s. The directions of colloid motion in the two fuels are shown in Figure 1.

Tapping mode atomic force microscopy showed no significant increase in the roughness of the Pd even after it was exposed to 10% N<sub>2</sub>H<sub>4</sub> for 70 min, thereby ruling out the role of Pd corrosion in the observed movement. Typical observations of colloid movements, in contrast, take less than 5 min.

It is hypothesized that the underlying mechanism at work in this system is analogous to the mechanism at play in the hydrogen peroxide-based pumping system described previously.<sup>5,7</sup> Briefly, the asymmetric decomposition of the hydrazine-derived fuels<sup>10</sup> sets up a concentration gradient of charged intermediates and thus an electric field along the metal surface. This electric field then induces an electroosmotic flow of fluid and an electrophoretic migration of tracer particles, the directions of which can either be the same or opposite depending on the ζ-potentials of the gold surface and the colloidal tracer. In regions of high electric field, that is, near the Pd disks, these electrokinetic forces are proportionally larger; and as expected, colloids can be seen to accelerate as they approach the Pd disks. The observed velocity of the colloids over small distances where the electric field is essentially constant can then be described by the Helmholtz–Smoluchowski equation (eq 1),

$$U = \frac{\epsilon J}{\sigma \eta} (\xi_p - \xi_w) \quad (1)$$

where U, ε, J, σ, η, ζ<sub>p</sub>, and ζ<sub>w</sub> are the observed colloid velocity, the permittivity of water, the current density between the two electrodes, the solution conductivity, the solution viscosity, the ζ-potential of the particle, and the ζ-potential of the metal surface. The ζ-potential of the Au surface may vary with time as the reaction

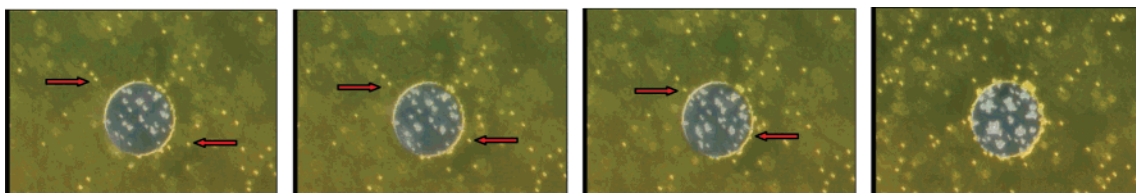


**Figure 2.** A 90  $\mu\text{m}$  diameter palladium disk on a gold surface: (left to right) images taken at 0, 2, 4, and 27 s after obtaining focus. Silica colloids (2.34  $\mu\text{m}$  diameter) can be seen moving inward toward the disk along the surface in a 611 mM  $\text{N}_2\text{H}_4$  solution.

**Table 1.** Mixed Potential Data (mV, vs Ag/AgCl, 3 M NaCl) for Pd and Au Ultramicroelectrodes (both 25  $\mu\text{m}$  in Diameter) in Aqueous 611 mM  $\text{N}_2\text{H}_4$  and 50 mM  $\text{N}_2\text{Me}_2\text{H}_2$

		Pd	Au
mixed potential in 611 mM $\text{N}_2\text{H}_4$	from Tafel plot	-651(15)	-310(15)
	from OCP	-630(25)	-345(28)
mixed potential in 50 mM $\text{N}_2\text{Me}_2\text{H}_2$	from Tafel plot	-70(20)	-283(16)
	from OCP	-58(15)	-265(14)

proceeds; however, it is assumed to be constant at a given distance from the Pd disk once the system has reached steady state. The  $\zeta$ -potential should be negative over the entire gold surface at pH 11, although some spatial variation created by the inhomogeneous current density distribution is possible.

In the systems described herein, the electroosmotic and electrophoretic velocities are always in opposite directions, with the electroosmosis in the same direction as the current. From eq 1, we can see that  $\zeta_P$  and  $\zeta_W$  of the same sign compete and drive motion in opposite directions. Choosing to use silica or amidine colloids results in the electrophoresis or the electroosmosis dominating, respectively, depending on the magnitude of the colloid  $\zeta$ -potential relative to that of the gold surface.

Supporting this hypothesis is the observation that when Pd and Au electrodes are in close proximity (10  $\mu\text{m}$ ) yet electrically isolated from one another, colloid motion along the gold surface is halted. As an additional test, a relatively nonpartitioning salt,<sup>11</sup>  $\text{KNO}_3$ , was added to the hydrazine system to increase the conductivity of the bulk solution. The speed of silica colloids was seen to decrease linearly with  $1/\text{conductivity}$ , as predicted eq 1. Upon addition of 10 mM  $\text{KNO}_3$ , colloid movement was decreased by 80%, whereas the measured current density only decreased by 22%; the latter decrease in activity can be rationalized as a slight poisoning of the catalytic surface by the salt.

Another test of the electrokinetic hypothesis is to determine the potentials at which the rates of the anodic and cathodic half reactions are exactly balanced for the relevant catalytic metal surfaces (here, Pd and Au).<sup>6</sup> At this "mixed potential" the net current is zero. If the mixed potential values are known for both metals comprising the micropump, then the direction of current flow, and thus the direction of electroosmosis, can be predicted.

Pd and Au ultramicroelectrodes were the working electrodes, and Ag/AgCl (3 M NaCl) was the reference electrode for these mixed potential measurements. The Au ultramicroelectrodes were circular disk electrodes made by polishing a 25  $\mu\text{m}$ -diameter Au wire sealed in glass. Pd ultramicroelectrodes were made by electroplating Pd onto the Au disk. The mixed potential was determined in two ways: by directly measuring the open circuit potential (OCP) and by performing slow voltammetric sweeps in the potential range of the anodic and cathodic half cell reactions (see Table 1). The mixed potentials were then obtained by extrapolating plots of  $\log|i|$  versus potential from the linear Tafel regions to their intersection, as illustrated in Figure 3. In aqueous  $\text{N}_2\text{H}_4$  solution, the mixed potential of Pd was more negative than

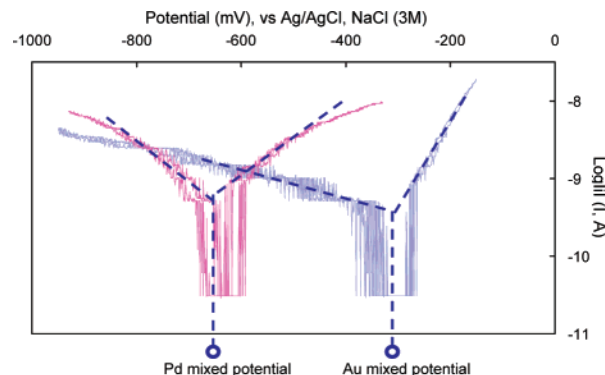


**Figure 3.** Tafel plots of Pd and Au ultramicroelectrodes in aqueous 611 mM  $\text{N}_2\text{H}_4$ . The intersection of the blue dotted lines corresponds to the mixed potential, indicated by circles on the potential axis.

that of Au, indicating that Au should act as the cathode. In  $\text{N}_2\text{-Me}_2\text{H}_2$  solution, the mixed potential of Au was more negative than that of Pd, indicating that Pd should be the cathode. In both cases, the direction of fluid flow and tracer particle motion were consistent with the sign of the mixed potential difference.

In summary, we have shown that hydrazine derivatives can be used as fuels for driving electrokinetic pumping and that the direction of fluid flow is fuel-dependent. These results suggest the possibility of using other redox-active fuels to power nanomotors, micropumps, and devices derived from them.

**Acknowledgment.** This work is supported by the Penn State Center for Nanoscale Science (NSF-MRSEC, DMR-0213623) and was performed in part at the Penn State Nanofabrication Facility, a member of the NSF National Nanofabrication Users Network

**Supporting Information Available:** Videos (mpg) and plots of movement of colloids in the presence of either  $\text{N}_2\text{H}_4$  or  $\text{N}_2\text{Me}_2\text{H}_2$ . This material is available free of charge via the Internet at <http://pubs.acs.org>.

## References

- (1) Paxton, W. F.; Kistler, K. C.; Olmeda, C. C.; Sen, A.; St. Angelo, S. K.; Cao, Y.; Mallouk, T. E.; Lammert, E.; Crespi, V. H. *J. Am. Chem. Soc.* **2004**, *126*, 13424–13431.
- (2) Dhar, P.; Fischer, T. M.; Wang, Y.; Mallouk, T. E.; Paxton, W. F.; Sen, A. *Nano Lett.* **2006**, *6*, 66–72.
- (3) (a) Fournier-Bidoz, S.; Arsenault, A. C.; Manners, I.; Ozin, G. A.; *Chem. Commun.* **2005**, 441–443. (b) Vicario, J.; Eelkema, R.; Browne, W. R.; Meetsma, A.; La Crois, R. M.; Feringa, B. L. *Chem. Commun.* **2005**, 3936–3938.
- (4) Kline, T. R.; Paxton, W. F.; Mallouk, T. E.; Sen, A. *Angew. Chem. Int. Ed.* **2005**, *44*, 744–746.
- (5) Kline, T. R.; Paxton, W. F.; Wang, Y.; Velegol, D.; Mallouk, T. E.; Sen, A. *J. Am. Chem. Soc.* **2005**, *127*, 17150–17151.
- (6) Wang, Y.; Hernandez, R. M.; Bartlett, D. J.; Bingham, J. M.; Kline, T. R.; Sen, A.; Mallouk, T. E. *Langmuir* **2006**, *22*, 10451–10456.
- (7) Paxton, W. F.; Baker, P. T.; Kline, T. R.; Wang, Y.; Mallouk, T. E.; Sen, A. *J. Am. Chem. Soc.* **2006**, *128*, 14881–14888.
- (8) Chang, S.; Paunov, V.; Petsev, D.; Velev, O. *Nat. Mater.* **2007**, *6*, 235–240.
- (9) Mano, N.; Heller, A. *J. Am. Chem. Soc.* **2005**, *127*, 11574–11 575.
- (10) Bard, A. J. *Anal. Chem.* **1963**, *35*, 1602–1607.
- (11) Saprykina, T. I.; Grushina, N. V.; Kozin, L. F. *Dvoynoi Sloi Adsorbts. Tverd. Elektrodakh* **1978**, *5*, 222–223.

JA0726512